HEFAT2014
10th International Conference on Heat Transfer, Fluid Mechanics and Thermodynamics
6 – 9 July 2014
Orlando, Florida

ON THE APPLICATION OF HOT WIRES AND PITOT TUBES IN PIPE AND CHANNEL FLOWS

E.-S. Zanoun[1,3], F. König[2], C. Egbers[2], E. Öngüner[2], F. Al Mutairi[3]
[1] Department of Mechanical Engineering, Faculty of Engineering, Benha University, Benha 71491, P.O. Box 741, Egypt
[2] Department of Aerodynamics and Fluid Mechanics (LAS), Brandenburg University of Technology (BTU-Cottbus), Siemens-Halske-Ring 14, D-03046 Cottbus, Germany
[3] Department of Mechanical Engineering, University of Tabuk, Tabuk 71491, P.O. Box 741, KSA
E-mail: elsayed.zanoun@aol.com

ABSTRACT

This paper looks mainly at two measuring techniques, namely, the hot-wire anemometer and the pitot tube when utilized in wall-bounded shear flows. Additional heat losses occur from the hot wires in presence of walls that are not accounted for in the calibration process of the wires. Because of this, corrections for erroneous in fluid velocity measured by the hot wire in the wall proximity are to be carried out. Similarly, when the pitot tube is applied to flow measurements, the mean shear gradient and the wall proximity come to play major roles of incorrect readings. Its size is therefore to be chosen such that corrections for the shear gradient and the wall proximity are minimal. The paper outlines, therefore, corrections applied to the pitot tube measured data in both pipe and channel flows. Available corrections are adopted in this paper to both the pipe and the channel flow measured data, yielding pitot tube results that are comparable to those of the hot wire and this was demonstrated by comparing the results corrected to the so-called the logarithmic velocity profile.

INTRODUCTION

Measurements of the local properties of turbulent flows in pipes and channels are of importance in theory and practical applications. Variety of measuring techniques, having finite volumes, e.g. the laser-Doppler anemometry (LDA), the hot-wire anemometer (HWA), and the pitot tube, are usually employed to carry out such local turbulence measurements. Some of these techniques provide volume-average information about the turbulent flow characteristics which might affect conclusions drawn from the resultant data. Few issues, hence, concerning the pipe and the channel mean flow measurements such as their dependence on the size of the control volume of the measuring technique still need more studies. New sets of pipe and channel data represent bases for the present research. A carefully designed pipe flow facility was constructed at the Department of Aerodynamics and Fluid Mechanics, Brandenburg University of Technology (BTU-Cottbus), providing the pipe flow data with the required fully developed flow properties [2]. On the other hand, the current channel flow data were obtained utilizing the channel flow facility at the Institute of Fluid Mechanics Erlangen Nürenberg (LSTM) [1].

Both the pipe and the channel flows have been investigated, utilizing hot wire, having small measuring control volume, e.g. wire diameter (d) of 5 μm and wire length (ℓ) of 1250 μm. In addition, intensive measurements using pitot tube, having inner and outer diameters of 0.25 mm, and 0.6 mm were carried out at streamwise locations of $L/H \approx 130$, and $L/D \approx 115$ for the pipe and channel, respectively.

The pipe experimental facility and the applications of the measuring techniques utilized are introduced briefly. The different methods adopted from the literature for correcting the pitot tube measurements for the shear gradient, and the blockage effects in the wall region are described. In addition, a comparative study between the pitot tube and the hot-wire results was conducted. Conclusions and outlooks are presented in the final section.

NOMENCLATURE

B	[-]	Log law additive constant
C_f	[-]	Channel skin friction coefficient
D/d	[m]	Pipe diameter/hot wire diameter
OD_{pitot}	[m]	Pitot tube outer diameter
ID_{pitot}	[m]	Pitot tube inner diameter
dP/dx	[Pa/m]	Mean pressure gradient along the test section
H	[m]	Channel full height
ℓ/ℓ_c	[m]	Hot wire length/flow characteristic length
L	[m]	Length of the pipe/channel test section
R	[m]	Pipe radius
R^+	[-]	The Kármán number
Re	[-]	The Reynolds number
U or V	[m/s]	Fluid mean velocity
u_τ	[m/s]	Wall friction velocity
W	[m]	Channel width
y	[m]	Wall distance

Special characters

τ	[N/m^2]	Shear stress
λ	[-]	Pipe friction factor
ν	[m^2/s]	Fluid kinematic viscosity
κ	[-]	von Kármán constant
ρ	[kg/m^3]	Fluid density
Δ	[m]	Centerline offset/displacement correction
δ	[m]	Boundary layer thickness

Subscripts

b	Bulk
c	Characteristics
m	Mean
w	Wall

EXPERIMENTAL FACILITY AND PROCEDURE

The department of aerodynamics and fluid mechanics (LAS) at the Brandenburg University of Technology (BTU-Cottbus) built the new pipe facility shown in Figure 1. The LAS CoLaPipe (**Co**ttbus **La**rge **Pipe**) is a relatively high Reynolds number test facility for various purposes ranging from basic to applied researches [2]. The CoLaPipe is closed-return facility with the suction side made of high-precision smooth Acrylic glass, having an inner pipe diameter of 190±0.23 mm and total length of 148 pipe diameter, i.e. $L/D\approx148$. The facility has a return pipe section made of smooth Acrylic glass with an inner diameter of 342±0.32 mm, and having $L/D\approx78$. It is worth noting that the facility is equipped with water cooler to keep the air temperature constant inside the facility test sections, i.e. the suction and the return lines. The temperature was measured with accuracy better than ±0.05°C

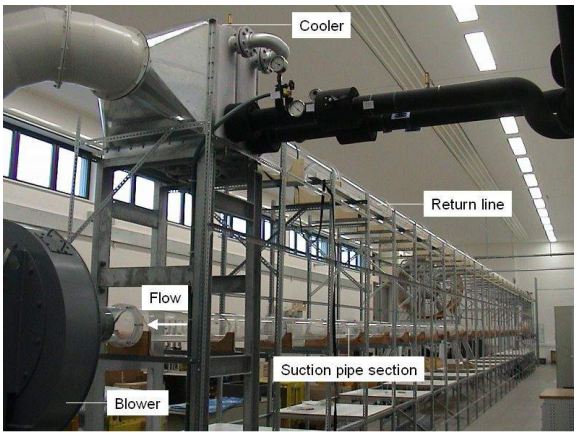

Figure 1 The CoLaPipe facility at LAS BTU-Cottbus.

The facility utilizes a powerful 45 kW radial blower to provide air with 80 m/s maximum speed at the contraction exit with turbulence intensity, $u'/U \le 0.5\%$. The maximum air speed achieved with the setup corresponds to approximately 0.23 Mach number, avoiding any compressibility effects. Aiming at a quite stable facility, the radial blower is located at the end of the pipe test section in the suction side and it delivers its output, directly, to the 342 mm diameter return line through a heat exchanger as shown in Fig. 1. It combines all the relevant components of the facility, see [2] for further details. This piece of work reports, therefore, on measurements of the mean velocity across the suction pipe section performed using the hot wire and the pitot tube. In addition, some new channel flow data obtained at LSTM Erlangen by Zanoun and Lukic are analyzed and presented.

A computer-controlled three dimensional high spatial resolution traverse system (Isel Germany AG) was used for traversing the hot wire and the pitot tube. The traverse is placed on scaled rail to facilitate its movement in streamwise, spanwise, and normalwise directions. Enough care was given to ensure a precise location of either the hot wire [3], or the pitot tube at a reference distance from the wall surface. The positioning absolute error with the present traverse mechanism was ±10 μm.

The mean velocity profiles and the mean wall pressure gradients along the pipe and channel test sections have been measured for various Reynolds numbers. The mean velocity profile measurements were carried out at a downstream distance 130D and 115H from the contraction exit for the pipe and channel, respectively. These lengths were considered to be sufficient to ensure the fully developed turbulent pipe and channel flows by reaching the measuring test section [4]. The pitot tube velocity measurements were made by traversing a total-head tube, having inner and outer diameters of ID_{pitot}= 0.25 mm, and OD_{pitot}=0.60 mm, respectively. The pitot tube is in accordance with recommendations by [5-7]. The dynamic head needed for velocity calculation was obtained by subtracting the static pressure from the total pressure measured by the total head tube. It is worth noting that the static pressure was obtained from a pressure tap on the pipe wall section corresponding to the pitot opening. Utilizing the Bernoulli equation, the pitot tube measurements were then converted to velocity. Each velocity profile was measured at 70 equally spaced vertical positions with particular care being given to the velocity distribution within the overlap region.

The hot wire velocity profile measurements were conducted using a 3.8 μm diameter wire, the TSI probe and anemometer. In addition, few runs have been carried out using a 5 μm diameter wire mounted on Dantec Constant Temperature Anemometer (CTA). All wires have aspect ratios of $\ell/d\ge200$. Measurements have been carried out for $1.75\times10^5\le Re_m\le9\times10^5$, and $4\times10^4\le Re_m\le2.4\times10^5$, for the pipe and the channel, respectively, where $Re_m = D\overline{U}_b/\nu$, $\overline{U}_b$ is the bulk flow velocity, D *is* the pipe inner diameter or the channel full height (i.e. $H\equiv D$), and ν is the air kinematic viscosity.

Figure 2 The Dantec calibration unit with the HWA probe.

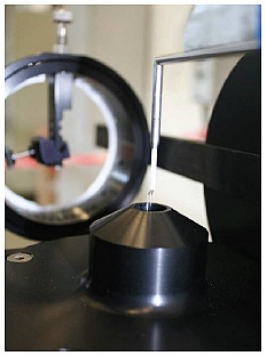

The hot-wire probes were calibrated before each set of measurements utilizing the Dantec calibration unit shown in Fig. 2. All calibrations and measurements were performed with an 80% overheat ratio. A fourth-order polynomial fit was the basis for the mean velocity estimation with an accuracy of better than ±1%.

The ambient air temperature inside the pipe section was kept constant. In case of an unavoidable temperature drift, instantaneous corrections were carried out during the calibration procedure as well as during measurements.

RESULTS AND ANALYSIS

It is essential for reliable investigations of the fully developed turbulent pipe and channel flows to estimate, accurately, the wall friction velocity (u_τ). This can be achieved by careful estimation of the wall shear stress via the measurements of the mean pressure gradient (dP/dx) along the pipe and/or the channel centerlines. To obtain the mean pressure gradient, the mean pressure was measured away from the pipe inlet (i.e. $L/D \geq 100$) at four different pressure locations, all being 1 m apart from each other. At each measuring location, three static pressure taps of 400 μm diameter were carefully installed around the circumference of the pipe. The mean static pressure at each location was obtained by averaging measurements of the three pressure taps and then the mean pressure gradient along the four meters was estimated having an accuracy better than ±0.25%. A similar approach was carried out for the channel flow. The wall friction velocity (u_τ), was then estimated as follows:

$$u_\tau = \sqrt{\tau_w/\rho}, \qquad where \tag{1}$$

$$Pipe: \ \tau_w = -\frac{R}{2}\frac{dP}{dx}, \qquad Channel: \ \tau_w = -\frac{H}{2}\frac{dP}{dx}$$

R is the pipe radius and H is the channel full height. Hence, the pipe friction factor, λ, and the channel skin friction, c_f, respectively, read as:

$$Pipe: \qquad \lambda = 8\left(u_\tau/\overline{U}_b\right)^2 \tag{2}$$

$$Channel: \qquad c_f = 2\left(u_\tau/\overline{U}_b\right)^2$$

As expected for the fully developed turbulent pipe flow at relatively high enough Reynolds numbers, the pipe friction data from the current pressure gradient measurements compares well with available friction relations and data as shown in Fig. 3.

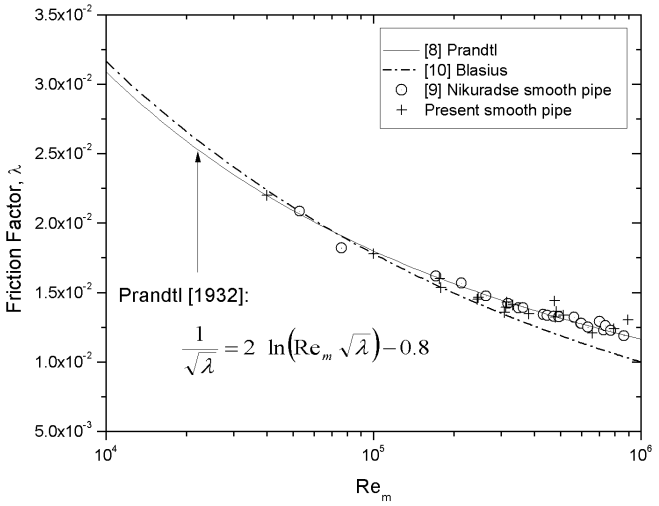

Figure 3 Pipe experimental friction data compared with data and formulae extracted from the literature.

A reasonable agreement was observed with Prandtl logarithmic friction relation for pipes [8], and with the experimental data of [9]. A good agreement with Blasius [10] for $Re_m<10^5$ was also obtained, however, for $Re_m>10^5$ a noticeable difference is observed and becoming larger for greater values of Reynolds number, here Re_m is based on the pipe diameter and the bulk flow velocity.

In channel flow, reliable wall skin friction data requires an assumption that the mean flow statistics are two dimensional. The two-dimensionality assumption is valid only if the channel has high enough aspect ratio, i.e. the ratio of the channel width to the channel full height (W/H) is greater than or equal to eight [1]. The set of data selected and presented in Fig. 4 is fulfilling the above assumption. Hence, the wall skin friction data obtained from the mean pressure gradient measurements along the channel centerline compared well with the logarithmic skin friction relation proposed by [1] as Fig. 4 shows.

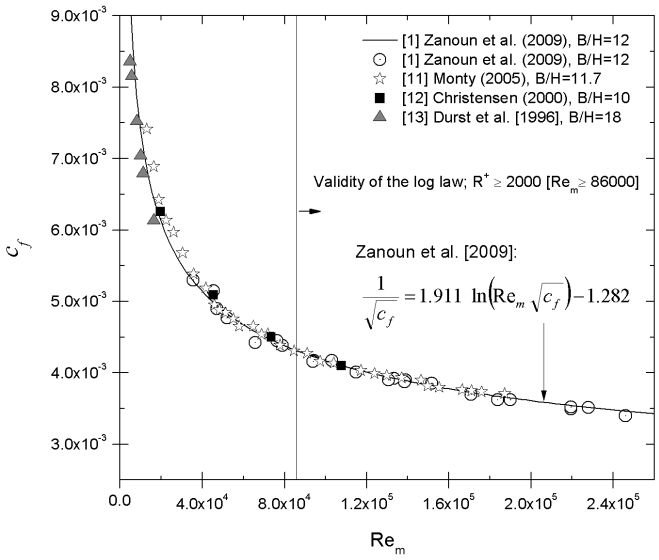

Figure 4 Channel skin friction from the literature compared to the logarithmic friction relation proposed by [1].

Few skin friction experimental data sets, e.g. of [11-13] for channel flows are represented in Fig. 4. The data of [11] were obtained via the mean pressure gradient measurements in plane channel, having an aspect ratio of 11.7:1 and for relatively high Reynolds number, $Re_m<2\times10^5$. The experimental data from [12], and [13], however, were for low Reynolds number range. Good agreement was observed among the different experimental data and with the logarithmic skin friction relation proposed by [1], in particular, for $R^+\geq2000$, where $R^+=0.5Hu_\tau/\nu$.

Pitot Tube versus Hot-Wire

In addition to the accurate estimation of the wall friction, the cross sectional mean velocity profile was measured. The pitot and/or the pitot-static tubes are, commonly, to be used to measure the total and/or the dynamic pressure, respectively, for the mean velocity calculations. It is, however, known, see e.g.

[14], that the presence of the pitot tube in shear flows causes changes in flow nature which can be summarized as follows:
1. Viscous effect: this effect is to be taken into consideration when $Re_{ODpitot}$<200, where $Re_{ODpitot}$ is the Reynolds number based on the pitot tube outer diameter and the bulk flow velocity.
2. Wall proximity effect (i.e. distortion of the velocity profile near a solid boundary): it is to be observed when the pitot tube is located within two-to-three diameters from the wall surface.
3. Velocity/shear gradient or displacement effect (see Fig. 5): this effect is due to:

(i) deflection of the incoming streamlines by the pitot tube (ii) the inequability of the average pressure measured by the pitot tube face to pressure measured at the geometric center of the tube, see [14] for more details.

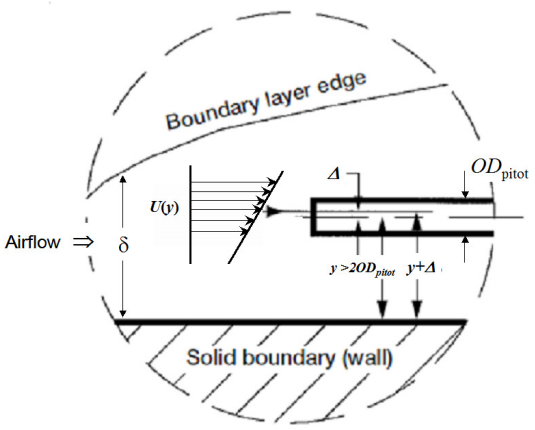

Figure 5 Illustration of the shear gradient or the centerline displacement effect when y>2OD_{pitot}, adopted from [14].

Figure 5 represents an illustration for the shear gradient effect or in other words the centerline displacement effect. The figure shows the offset Δ of the effective center of the pitot tube displaced from the geometric center towards the region of the higher velocity, i.e. displacing the boundary layer velocity profile by Δ to the higher velocity direction. Thus the offset is compensating for the higher velocity streamlines deflected towards the gradient effect as illustrated in Fig. 5, see [14 &15].

Of the three above listed effects, the velocity/shear gradient effect is most predominant in the wall-bounded shear flows. It has been the goal of a number of earlier and recent researchers, see e.g. [6-7, 14-18] and part of the current research work to better understand the nature of the centerline displacement effect in order to compensate for it.

Hence, it is of crucial importance when the pitot tube is used for velocity measurements, its tube size is to be considered and its influence on the mean velocity is to be, however, better expressed in terms of the wall units. Measurements were carried out using the pitot tube, having an outer diameter of 0.6 mm in addition to the hot-wire anemometry. The wall friction velocity, u_τ, and the viscous length, $\ell_c = \nu/u_\tau$, scales were used to represent the results in general form,, i.e. representing the mean velocity distribution in the form of $U^+ = f(y^+)$.

It is recommended by [14] that the viscous effect is to be taken usually into consideration when 30<$Re_{ODpitot}$<200. For the current work, the corrections for the viscous effect is neglected since the lowest value for the Reynolds number was beyond the upper limit, i.e. $Re_{ODpitot}$<200, for neglecting the viscous effect. A sample of the uncorrected pitot-tube mean velocity profiles is illustrated in Fig. 6(a) and (b), compared with the hot-wire mean velocity profiles. A displacement effect, i.e. velocity overshoot, was clearly observed in the region where y^+<200 in the pipe and for y^+<150 in the channel, resulting in disagreement between the pitot tube and the hot-wire results. However, it was noticed that the pitot tube measured velocity profile for y^+>300 for pipe and for y^+>150 in channel showed satisfactory agreement with the hot-wire data along the overlap region and with the following logarithmic line:

$$U^+ = \frac{1}{\kappa}\ln y^+ + \mathrm{B} \qquad (3)$$

having κ = 0.384 and B = 4.43 for a pipe flow with log interval y^+=300–0.15R^+, see [19], and κ = 0.37 and B = 3.7 for a channel flow with log interval y^+=150–0.2R^+, see [1].

The pitot tube produces an overshoot in the mean velocity distribution in both the pipe and the channel flows when the measuring tube is located around the buffer region, 5<y^+<300 , as can be observed from Fig. 6. Comparing Fig. 6a with Fig. 6b, one could observe weaker velocity overshoot in the channel flow than the pipe flow. This might be attributed to the fact that the inner-region structure for the pipe flow is more complex than that for the channel flow.

The overshoot observed in the channel flow by [20] utilizing the laser Doppler anemometry was interpreted as an effect for the low Reynolds number range, making the data to depart from the logarithmic velocity profile, see also [4]. On the other hand, the velocity overshoot in the pipe flow was interpreted as part of the velocity distribution which can be represented by a power law [21]. A significant error in measurements also resulted because of the wall interference in case of the pitot tube was placed close to the wall, i.e. for wall distances less than two-to-three tube diameters which in terms of the wall units corresponds to y^+≈100–170 in the present study for the two cases presented for pipe and channel.

The overshoot observed in velocity profiles might be a reasonable justification for the higher values of the constants of the logarithmic velocity profile obtained when the pitot tubes are being used for velocity measurements, in particular, if the inner limit of the log law was considered to be y^+=30, see Tables 1 and 2. In addition, the velocity obtained by the pitot tube measurements is calculated after an averaging process of pressure measurements, resulting in erroneous in fluid velocity measured because of the quadratic non-linearity of the averaging process and calculation. In contrast, an instantaneous transformation of voltage measurements was carried out when using the hot wire before velocity calculation. Moreover, the pitot tube show problems due to the velocity fluctuations, in particular, in the wall layer.

Hence, when the pitot tubes are to be utilized to measure the mean velocity in the wall proximity their sizes have to be chosen such that the shear gradient, and blockage effects are

minimized. In addition, the effect of the near-wall high turbulence level is to be considered.

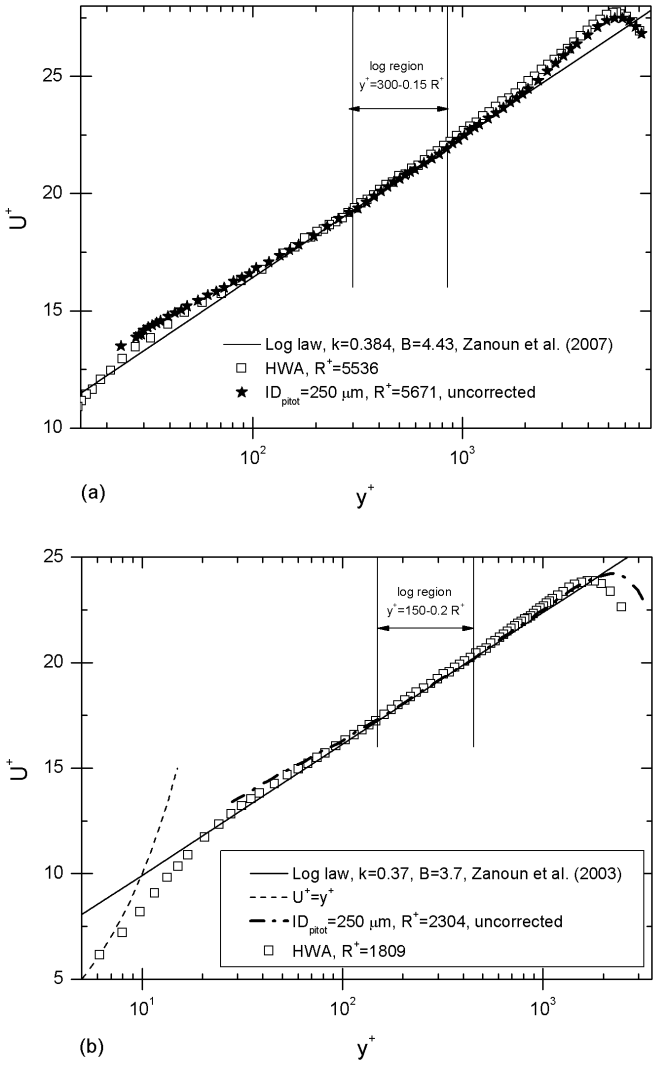

Figure 6 The hot wire and the uncorrected pitot tube mean velocity profiles in comparison with the logarithmic lines in **(a)** pipe, and **(b)** channel.

Variety of corrections for the pitot tube readings were found in the literature. Corrections, therefore, for the shear gradient, blockage, and wall turbulence were carried out for two Reynolds numbers, i.e. $Re_m \approx 2.8\times10^5$ (R^+=5671) and $Re_m \approx 1.02\times10^5$ (R^+=2304) for the pipe and the channel flows, respectively. For instance, to account for the shear gradient effect, MacMillan [16] introduced a correction factor for the pitot tube measurements by shifting the wall vertical coordinates towards the higher velocity region by $\Delta=0.15OD_{pitot}$, where Δ is called the displacement correction factor. It is worth noting that MacMillan's displacement correction is only applicable for wall distances beyond two pitot diameters, i.e. the pitot is located at a distance which is greater than $2OD_{pitot}$ from the wall surface. Therefore, it seems at the first glance that it is easy to correct the pitot tube data for the shear gradient effect by adding $0.15OD_{pito}$ to the y-coordinates. However, this displacement correction is dependent not only on the pitot tube outer diameter but also on the magnitude of the velocity gradient and the distance from the wall. Therefore, to avoid the constant shift for the pitot tube measured data, Hall [23] and Lighthill [24] proposed a displacement correction (Δ) as a function of the pitot tube diameter and the local velocity gradient which reads as

$$\varepsilon = \frac{\Delta}{OD_{pitot}} = 0.15\tanh(4\sqrt{\alpha}) \tag{4}$$

where the shear parameter α is given by

$$\alpha = OD_{pitot}\frac{dU/dy}{2U} \tag{5}$$

and evaluated at the geometric center of the pitot tube. The above displacement correction proposed by [24] was adopted to correct the present pipe and channel pitot-tube measurements.

In addition to the displacement correction discussed above, an additional correction is also required for wall distances less than $2OD_{pitot}$ from the wall. So, for wall distances $y<2OD_{pitot}$, MacMillan [16] observed the wall effect on the pitot tube measurements and proposed a correction curve presented in Fig. 8 in his paper in 1956. The mechanism of the wall proximity effect on the pitot tube readings was, however, explained by [18] as it resembles a forward-facing step causing the streamlines to be displaced away from the wall towards the region of a higher velocity. Therefore, based on MacMillan's wall correction curve [16], the so-called velocity correction (i.e. wall term) was proposed by [18], taking the following form:

$$\frac{\Delta U}{U} = 0.015\exp\left[-3.5\left(\frac{y}{OD_{pitot}}-0.5\right)\right] \tag{6}$$

It is to be used to correct the measured velocity for wall distances $y < 2\ OD_{pitot}$. The corrections discussed above for the shear and the wall effects were applied for a sample of the current pipe and channel flow measurements and the outcome is presented in Fig. 7.

The outer diameter of the pitot tube utilized in the present study was 0.6 mm which was equivalent to $y^+\approx$46-56 in terms of the wall units for the two cases presented in both Figs. 6 & 7. An appropriate correction approach is usually to be judged by a good collapse of the pitot tube data corrected with the hot wire measurements. By looking at Fig. 7, a conclusion might be drawn that the pitot tube corrected data have plausible agreement with the hot wire data. When it comes to analyze the law of the wall, in particular, with consideration of the inner limit of the logarithmic law, it becomes a critical issue taking into account the data points within the $2OD_{pitot}$ from the wall, i.e. $y^+\leq200$. It appears from Fig. 7 that for wall distances $y^+\leq200$ the pitot tube data suffers from both the shear gradient and the wall effects. When the uncorrected data for the wall distances $y^+\leq200$ was used in the analysis of the logarithmic velocity profile, few questions might be raised. For instance, utilizing the uncorrected data and considering the inner limit of the logarithmic line y^+=30, which was the most common inner

limit for many years before the last two decades, the outcomes, κ=0.419 and B=5.82, are not surprising to be in full agreement with [9] (i.e. κ=0.417 and B=5.84). On the other hand, carrying out the same analysis utilizing the corrected data set while keeping the inner limit of the log range to be y^+=30, reductions of 4.7% in the value of the von Kármán constant (κ=0.399) and around 13% in the additive constant (B=5.084) were obtained. On the contrary, based on the recent analysis of the logarithmic law of the wall, see. e.g. [19, 21], and with considering the inner limit to be $y^+\approx$300 which is beyond the strong effect of the wall, lower values for both constants of the logarithmic line were obtained, showing good agreement with recent values obtained by [19 & 25].

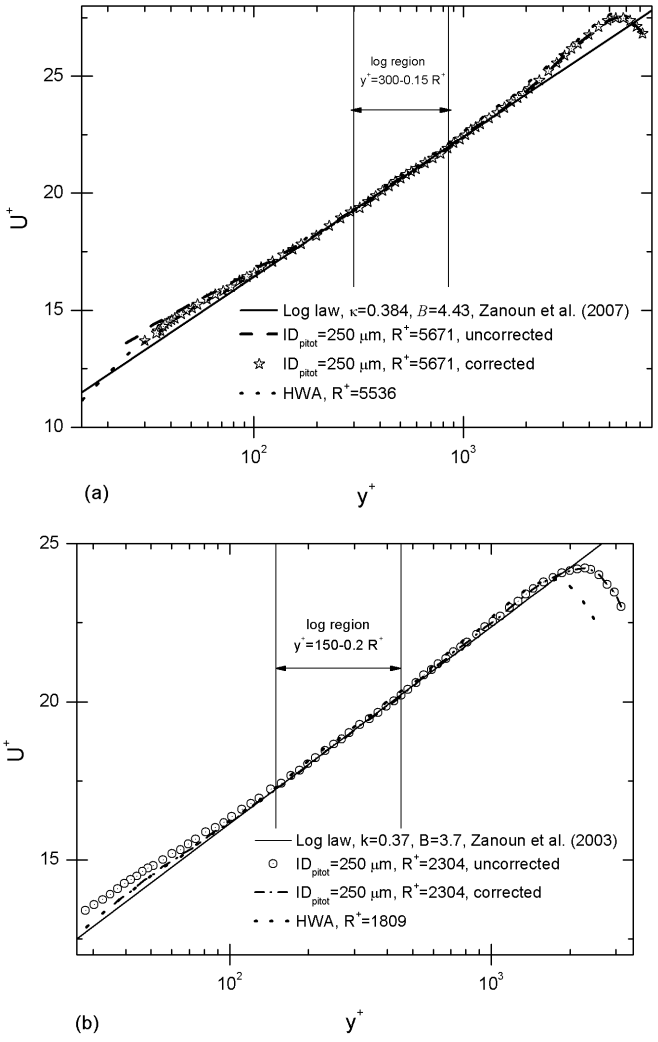

Figure 7 The corrected versus uncorrected pitot tube mean velocity profiles, compared with the logarithmic line and hot wire data, **(a)** pipe flow, **(b)** channel flow.

More analysis of the data presented in both Fig. 6 & 7 results in new and useful outcomes, summarized and presented in Tables 1 and 2.

Table 1: Summary of the pipe log-law constants for different log ranges utilizing the pitot tube results for R^+=5671.

Log range	without correction		with correction	
$y^+ = (y^+_{inner} - y^+_{outer})$	κ	B	κ	B
$y^+ = 30 - 0.15\ R^+$	0.419	5.82	0.399	5.084
$y^+ = 300 - 0.15\ R^+$	0.393	4.76	0.389	4.603

Table 2: Summary of the channel log-law constants for different log ranges utilizing the pitot tube results for R^+=2304.

Log range	without correction		with correction	
$y^+ = (y^+_{inner} - y^+_{outer})$	κ	B	κ	B
$y^+ = 30 - 0.2\ R^+$	0.409	5.16	0.383	4.23
$y^+ = 150 - 0.2\ R^+$	0.381	4.15	0.372	3.77

CONCLUSIONS AND FINAL REMARKS

Pitot tube results, uncorrected and corrected for the shear gradient and the wall proximity, were presented and compared with results obtained by the hot-wire anemometer. The conclusions drawn from the results and discussions in the different sections may be summarized as follows:

The data set discussed above suggests that the dynamic response of the pitot tube in turbulent shear flows still need more and careful analysis to fully understand the overall corrections, minimizing the viscous, the shear gradient, the wall proximity, and the turbulence effects. However, the authors noticed that even without applying corrections, the evaluation of the von Kármán constant by fitting the data starting from y^+=300 or y^+=150 for the pipe and channel, respectively, using the pitot tube with small diameter, i.e. ID_{pitot}<250μm, resulted in values comparable to those obtained from the hot wire results either in the pipe or the channel flows.

The authors are, however, recommending future use of the displacement correction embodied in (4.1) and proposed by [15]. In addition, further study to understand the effect of the pitot tube corrections on the scaling laws and on values of the constants of the logarithmic velocity profile is needed. It is also worth paying more attention to other measuring techniques, e.g. the laser Doppler anemometry, that would help more resolving the wall layer of the wall-bounded shear flows with better resolution.

ACKNOWLEDGMENT

The authors' gratefully acknowledge the support received from both the Institute of Fluid Mechanics (LSTM) Erlangen-Nürenberg and the Department of Aerodynamics and Fluid Mechanics (LAS), BTU-Cottbus.

REFERENCES

[1] Zanoun, E.-S., Durst, F., Nagib, H., "Refined C_f relation for turbulent channels and consequences for high Re experiments," J. Fluid Dyn. Res. 41, 1-12, (2009).

[2] Zimmer, F., Zanoun, E.-S., Egbers, C., "A study on the influence of triggering pipe flow regarding mean and higher order statistics," Journal of Physics: Conference Series 318 (2011) 032039 doi:10.1088/1742-6596/318/3/032039.

[3] Durst, F., and Zanoun, E.-S., "Experimental investigation of near-wall effects on hot-wire measurements," Exp. Fluids 33, pp. 210-218, 2002.
[4] Zanoun, E.-S., Kito, M., and Egbers, C., "A study on flow transition and development in Circular and Rectangular Ducts," J. Fluids Eng. 131, 061204, June 2009.
[5] Bryer, D.W., and Pankhurst, R. C., "Pressure-probe methods for determining wind speed and flow direction," Nat. Phys. Lab., London, 1971.
[6] Sami, S., "The Pitot tube in turbulent shear flow," Proc. 11th Midwestern Mech. Conf., Dev. in Mechanics, Vol. 5, Paper 11, pp. 171, 1967.
[7] Chue, S. H., "Pressure probes for fluid measurements," Pro. Aero. Sci., 16, 2, pp. 147-223, 1975.
[8] Prandtl, L., "Reibungswiederstand, hydrodynamische Probleme des Schiffsantriebs," herausgeg, v. G. Kempf u. E. Förster 1932 S. 87; – Neuere Ergebnisse der Turbulenzforschung, Z. VDI Bd. 77 (1933) Nr. 5 S. 105; – Ergebnisse der Aerodynamischen Versuchsanstalt Göttingen, 3 Lief. (1927) S. 1, (English Translation NACA TM 720).
[9] Nikuradse, J., "Gesetzmässigkeiten der turbulenten Strömung in glatten Rohren," Forschg. Arb. Ing.-Wes. 356, 1932.
[10] Blasius, "Über Flüssigkeitsbewegung bei sehr kliner Reibung," Proc. Third Int. Math. Congr., Heidelberg: pp. 484‑491, 1908.
[11] Monty, J. P., 2005, "Developments In smooth wall turbulent duct flows," PhD Thesis, The University of Melbourne, Australia.
[12] Christensen, K. T., 2001, "Experimental investigation of acceleration and velocity fields in turbulent channel flow," PhD thesis, Department of Theoretical and Applied Mechanics, University of Illinois at Urbana-Champaign, USA.
[13] Durst, F., Kikura, H., Lekakis, I., Jovanovic, J., Ye, Q.-Y. 1996, "Wall shear stress determination from near-wall mean velocity data in turbulent pipe and channel flows," Exp. Fluids 20(6), pp. 417-428.
[14] Grosser, W. I., "Factors Influencing Pitot Probe Centreline Displacement in a Turbulent Supersonic Boundary Layer," NASA Technical Memorandum 107341, January 1997, pp. 1-47.
[15] Bailey, S. C. C., Hultmark, M., Monty, J. P., Alfredsson, P. H., Chong, M. S., Duncan, R. D., Fransson, J. H. M., Hutchins, N., Marusic, I., McKeon, B. J., Nagib, H. M., Orlue, R., Segalini, A., Smits, A. J., and Vinuesa, R., "Obtaining accurate mean velocity measurements in high Reynolds number turbulent boundary layers using Pitot tubes," J. Fluid Mech. (2013), vol. 715, pp. 642-670.
[16] MacMillan, F. A., "Experiments on Pitot-tubes in shear flow," Aero. Res. Counc. R. & M. 3028, 1956.
[17] Tavoularis, S., "Techniques for turbulence measurements," Encycl. Fluid. Mech. Vol. 1, Flow Phenomena and Measurement, pp. 1207-1255, 1986.
[18] McKeon, B. J., Li, J., Jiang, W., Morrison, J. F., and Smits, A. J., "Pitot probe corrections in fully developed turbulent pipe flow," Meas. Sci. Technol. 14, pp. 1449-1458, 2003.
[19] Zanoun E. S., Durst F., Saleh O., and Al-Salaymeh A., "Wall Skin Friction and Mean Velocity Profiles of Fully Developed Turbulent Pipe Flows," Exp. Therm. Fluid Sci. 32(1), pp. 249–261, 2007.
[20] Fischer, M., "Turbulente wandgebundene Str¨omungen bei kleinen Reynoldszahlen," Dissertation, Universit¨at Erlangen Nürnberg, 1999.
[21] Zagarola, M. V., and Smits, A. J., "Mean-flow scaling of turbulent pipe flow," J. Fluid Mech. 373, pp. 33-79, 1998.
[22] Gad-el-Hak, M., "Basic instruments," The Handbook of Fluid Dynamics, CRC Press, Part V (33), pp. 1-22, 1998.
[23] Hall, M. I., "The displacement effect of a sphere in two-dimensional shear flow," *J. Fluid Mech.* 1, 1956, 142–62.
[24] Lighthill, M. J., "Contributions to the theory of the Pitot-tube displacement effect," J. Fluid Mech. 1 493–512, 1957.
[25] Perry, A. E., Hafez, S., Chong, M.S., "A possible reinterpretation of the Princeton superpipe data," J. Fluid Mech. 439, pp. 395-401, 2001.